

# Indirect tests of the Randall-Sundrum model

**Sandro Casagrande**

Excellence Cluster Universe, Technische Universität München  
D-85748 Garching, Germany

E-mail: [sandro.casagrande@ph.tum.de](mailto:sandro.casagrande@ph.tum.de)

**Abstract.** I present phenomenological implications of the Randall-Sundrum model for indirect searches, specifically a selection of flavor observables and Higgs-related collider searches. I review the interplay of constraints from CP violation in flavor physics, possible effects in rare decays, and model-specific protection mechanisms. Deviations in the Higgs couplings to fermions and, at one-loop, to gluons are unexpectedly strong and lead to strong modifications in Higgs searches.

## 1. Introduction

The gauge hierarchy problem is one of the driving theoretical reasons for the invention and necessity of new physics at the electroweak scale. Its strength can be quantified as a technical naturalness problem induced by the instability of the electroweak scale under radiative corrections, which gains severity given the hierarchy of 16 orders of magnitude between the electroweak and the Planck scale  $M_{\text{PL}}$ . Models with compact extra dimensions explain this hierarchy in terms of geometry, and at the same time also the hierarchical structures observed in the fermionic masses and mixing angles via so-called geometrical sequestering [1].

This can be achieved naturally within the framework of a warped extra dimension, first proposed by Randall and Sundrum (RS) [2]. There one studies the Standard Model (SM) on a background consisting of Minkowski space, embedded in a slice of five-dimensional anti de-Sitter geometry ( $AdS_5$ ) with curvature  $k$ . The fifth dimension is an  $S^1/Z_2$  orbifold of size  $r$ , and has two branes located at orbifold fixed points, the UV and the IR brane. The geometry is given by

$$ds^2 = e^{-2\sigma(\phi)} \eta_{\mu\nu} dx^\mu dx^\nu - r^2 d\phi^2, \quad \sigma(\phi) = kr|\phi|, \quad (1)$$

where  $e^{\sigma(\phi)}$  is called the warp factor. For  $L \equiv kr\pi \equiv -\ln(\epsilon) \approx \ln(10^{16})$  the exponential contraction of length scales along the extra dimension mediates between a physical scale  $M_{\text{KK}} \equiv k' \equiv k\epsilon \sim \text{TeV}$  and a fundamental scale  $k \lesssim M_{\text{Pl}}$ . We use the common setup of allowing the gauge and matter fields to spread in the  $AdS_5$  bulk. This SM-like 5d gauge theory is the minimal setup from the dual conformal field theory point of view, as it implies that only the Higgs is a total TeV-scale composite of the strongly interacting sector, while SM gauge fields are fundamental and SM fermions are mostly fundamental with small mixing to the conformal sector [3]. Pragmatically thought, we only protect the scalar mass, leaving masses of higher-spin fundamentals to be protected by chiral or gauge symmetries.<sup>1</sup>

Fermions in the bulk admit a natural explanation of the flavor structure of the SM [5, 6, 7]. We achieve this by exponential localization of the fermion zero modes, which are the lowest

<sup>1</sup> For a more exhaustive review on the development of the model see [4] and the references therein.

mass harmonics of the 5d fermions. They receive their physical mass only from effective Yukawa couplings, resulting from their wave-function overlap with a Higgs boson. The latter is confined very close to the IR brane, where we may use the limit of complete localization for simplicity. The fermionic IR brane value  $F(c)$  is exponentially suppressed by the volume factor  $L$ , if the normalized bulk mass parameters  $c_{Q_i} = +M_{Q_i}/k$ , and  $c_{q_i} = -M_{q_i}/k$  are smaller than a critical value  $-1/2$ . Otherwise  $F(c)$  is of order one. Here  $M_{Q_i}$  and  $M_{q_i}$  denote the masses of the five-dimensional  $SU(2)_L$  doublet and singlet fermions. The exponential hierarchies are used to generate a hierarchical Yukawa matrix out of anarchical  $\mathcal{O}(1)$  fundamental Yukawa coupling

$$\mathbf{Y}_q^{\text{eff}} = \text{diag}(F(c_{Q_i})) \mathbf{Y}_q \text{diag}(F(c_{q_i})), \quad F(c) \approx \exp(\min(c + 1/2, 0)L) \sqrt{1 + 2c}. \quad (2)$$

The model features a plethora of higher harmonics above the TeV scale, the KK excitations of gauge bosons starting at  $m_{g^{(1)}} \approx 2.45 M_{\text{KK}}$ , graviton  $m_{G^{(1)}} \approx 3.83 M_{\text{KK}}$ , etc. each followed by an infinite tower of states, and additional mixings with the SM fields. Yet it is determined by a rather small set of new parameters [8], *e.g.* in the quark sector we have 18 additional moduli and 9 phases. Moreover, explaining the SM fermion spectrum constrains all ratios of the values  $F(c)$ . *E.g.* in the quark sector [4, 7, 9], up to  $\mathcal{O}(1)$  factors

$$m_{q_i} \sim \frac{v}{\sqrt{2}} F(c_{Q_i}) F(c_{q_i}), \quad \lambda \sim \frac{F(c_{Q_1})}{F(c_{Q_2})}, \quad A\lambda^2 \sim \frac{F(c_{Q_2})}{F(c_{Q_3})}, \quad (3)$$

leading to the numerical distribution shown in figure 1, where we used exact formulas [4]. Thus

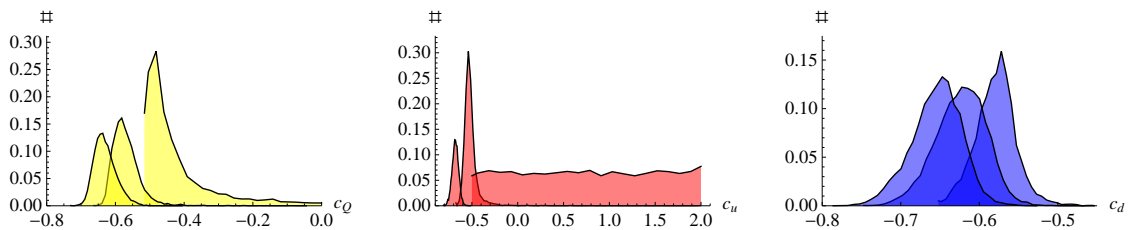


**Figure 1.** Distribution of bulk masses for  $M_{\text{KK}} \in [1, 10]$  TeV,  $\epsilon = 10^{-16}$ , and flat  $c_{t_R}$  prior.

the model has well testable predictions, which could be observed in future measurements, yet we have to assure conformity with existing measurements. Most prominently, the compliance with electroweak precision data tightly restricts the minimal model to  $M_{\text{KK}} > 4.0$  TeV at 99% CL [10, 4]. There exist several ways to relax this constraint, like a possible high Higgs mass of about 1 TeV, which would be natural in this model and cancels the model-dependent contribution to the  $T$  parameter, leading to a lower bound  $M_{\text{KK}} > 2.6$  TeV. Also restricting the model to warp only up to an intermediate and safe UV scale can help to lower the bound (see [11] for restrictions of this approach). Alternatively one can make use of the custodial  $O(4)$  symmetry of the Higgs sector, by extending the bulk hypercharge group to  $SU(2)_R \times U(1)_X$ , breaking it to  $U(1)_Y$  on the UV brane by specific orbifold boundary conditions [3]. The Higgs mechanism on the IR brane may safely break  $SU(2)_L \times SU(2)_R$  to the diagonal  $SU(2)_V$  subgroup. This suppresses tree level contributions to  $T$  by three orders of magnitude and implies  $M_{\text{KK}} > 2.4$  TeV, which can even be lowered further by calculable fermionic loop contributions to  $T$ .<sup>2</sup> A discrete left-right parity symmetry and specifically chosen fermion representations [13] furthermore relax constraints from the precisely measured  $Zb\bar{b}$  vertex allowing for a wide range of right handed bottom and left handed top/bottom bulk masses, even for a low new physics scale.

<sup>2</sup> However, quark bi-doublets necessary to protect  $Zb_L\bar{b}_L$  typically tend to give a negative contribution to  $T$ , which would even raise the bound [12].

It is well known that strong constraints on the parameter space of new physics models can also arise from flavor observables. Depending on the flavor structure and the first quantum order of flavor changing neutral currents, this translates into a bound on the new physics scale, and might result in a tension to the resolution of the hierarchy problem. This is the so called flavor puzzle, which is partly addressed in the RS model in the way fermion hierarchies are generated. The mechanism is referred to as the RS-GIM and we show its numerical implications below.

Given the relatively high bounds on the scale  $M_{\text{KK}}$  and consequently on new particles, we consider it worthwhile to present possibilities which might indirectly allow for detection or exclusion of a warped extra dimension. We start at the high luminosity frontier with effects on flavor observables, emphasizing the most prominent bound coming from indirect CP violation (CPV) in  $K-\bar{K}$  transitions. We show that also direct CPV provides an effective constraint on some rare decays and discuss selected correlations, based on the exhaustive survey [11]. At the high energy frontier we present a recent full one-loop calculation of the effect in Higgs production and decays [14], which shows in strong shifts in the feasibility of Higgs searching strategies.

Since the RS-GIM mechanism implies flavor dependent couplings ordered with the fermion masses, it is most reasonable to expect changes in top couplings. This could affect for instance the forward-backward asymmetry in  $t\bar{t}$  production, for which the measurement by CDF has very recently been affirmed [15], and a significant deviation from the NLO QCD prediction in the high invariant mass region has been found. However one must carefully account for the explanation of the flavor structure. The latter renders the leading-order axial-vector couplings to the KK-gluon dominated contributions far too small to explain the discrepancy, and also the interference of vector couplings with the one-loop SM diagrams is outweighed by the leading-order contribution to the symmetric cross section  $\sigma_{t\bar{t}}$  [16]. Another coupling of the top quark, namely to a Higgs boson and a charm quark, receives enhanced importance [17] for which we show numerics to round off this presentation.

## 2. Flavor related effects and constraints

Indirect CPV in  $K \rightarrow \pi\pi$  decays has an outstanding constraining power in many extensions of the SM. It is induced by  $K - \bar{K}$  transition and the most recent theoretical determination of the imaginary value of the corresponding transition amplitude is given by  $\epsilon_K = (1.90 \pm 0.26) \cdot 10^{-3}$  [18]. In the effective-theory parametrization

$$\mathcal{H}_{\text{eff}}^{\Delta S=2} = \sum_{i=1}^5 C_i Q_i^{sd} + \sum_{i=1}^3 \tilde{C}_i \tilde{Q}_i^{sd}, \quad (4)$$

helicity structures beyond the  $V-A$  couplings of charged SM currents can contribute to the amplitude. Most importantly  $Q_4 = (\bar{d}_R s_L)(\bar{d}_L s_R)$ , can be generated by the exchange of new colored particles. Its coefficient enters the approximate formula for the  $K-\bar{K}$  mixing amplitude

$$\langle K^0 | \mathcal{H}_{\text{eff,RS}}^{\Delta S=2} | \bar{K}^0 \rangle \propto C_1^{\text{RS}} + \tilde{C}_1^{\text{RS}} + 114.8 \left( 1 + 0.14 \ln \left( \frac{\mu_{\text{KK}}}{3 \text{ TeV}} \right) \right) \left( C_4^{\text{RS}} + \frac{C_5^{\text{RS}}}{3.1} \right). \quad (5)$$

We observe that  $C_4^{\text{RS}}$  has a large coefficient, which originates from the chiral enhancement of the hadronic matrix elements, and the RG evolution down to 2 GeV. Thus the strongest contribution comes from KK-gluon exchange [9, 19, 20]. The RS-GIM is at work, as each fermion attached to a flavor violating vertex contributes approximately a factor of its IR brane value  $F(c)$  leading to  $C_4^{\text{RS}} \sim \frac{8\pi\alpha_s}{M_{\text{KK}}^2} L F(c_{Q_1}) F(c_{Q_2}) F(c_{d_1}) F(c_{d_2})$ .

In figure 2 we observe that the median value of  $|\epsilon_K|$  is consistent with the measurement only for  $M_{\text{KK}} \gtrsim 8 \text{ TeV}$ . However the 5% quantile crosses the experimentally allowed range already at about 2 TeV. The slow decoupling therefore introduces a moderate amount of arbitrariness

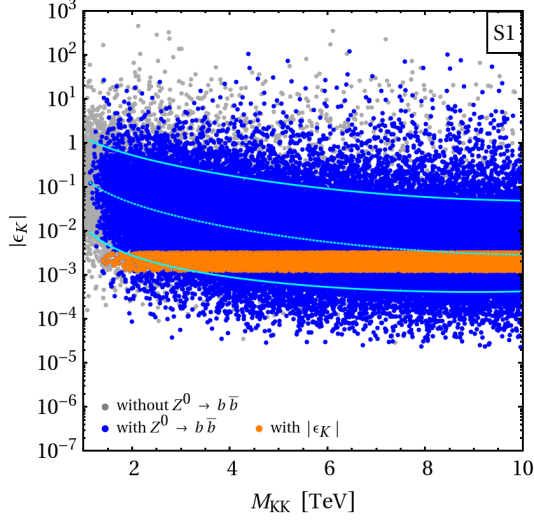


**Figure 2.** Prediction for  $|\epsilon_K|$  in the setup with minimal field content. All points reproduce the observed fermion spectrum, and CKM matrix, are not excessively fine-tuned, and have perturbative Yukawa couplings up to the 2<sup>nd</sup> KK-level. Points colored blue are consistent with  $Z^0 \rightarrow b\bar{b}$  at the 99% CL, and orange points fall inside the experimental 95% CL of  $|\epsilon_K|$  combined with the theory error. The cyan lines illustrate the decoupling behavior obtained from a fit to the 5%, 50%, and 95% quantile.

in the definition of a bound on the new physics scale inferred from this observable, and it is important to be aware of the different quality compared to the aforementioned bounds from electroweak precision observables.

One possibility to protect  $|\epsilon_K|$  from excessive corrections is to arrange for common bulk mass parameters in the sector of the right-handed down-type quarks [21]. In [20] we showed that the typical suppression of  $C_4^{\text{RS}}$  amounts to a factor of  $8 \cdot 10^{-3}$  and discuss a few other resolutions.

The hadronic uncertainties involved in direct CPV in  $K \rightarrow \pi\pi$  are larger compared to those in  $\epsilon_K$ . Yet it turns out to be useful to look at  $\epsilon'_K/\epsilon_K$ , which describes the ratio of direct over indirect CPV in this decay and is defined in terms of ratios of  $\Delta I = 3/2$  and  $\Delta I = 1/2$  transitions

$$\frac{\epsilon'_K}{\epsilon_K} = \frac{1}{\sqrt{2}} \left( \frac{A(K_L \rightarrow (\pi\pi)_{I_2})}{A(K_L \rightarrow (\pi\pi)_{I_0})} - \frac{A(K_S \rightarrow (\pi\pi)_{I_2})}{A(K_S \rightarrow (\pi\pi)_{I_0})} \right). \quad (6)$$

Taking into account the SM Wilson coefficients and the renormalization-group evolution from  $\mu_W$  to  $\mu_c$  [22, 23] we observe that contributions to the QCD penguin and the electroweak penguin

$$Q_6 = 4 (\bar{s}_L^\alpha \gamma^\mu b_L^\beta) \sum_q (\bar{q}_R^\beta \gamma_\mu q_R^\alpha), \quad Q_8 = 6 (\bar{s}_L^\alpha \gamma^\mu b_L^\beta) \sum_q Q_q (\bar{q}_R^\beta \gamma_\mu q_R^\alpha), \quad (7)$$

play the dominant role [20]. Indeed, both QCD and electroweak penguin contributions generated at a high scale are strongly enhanced by the RG evolution from  $\mu_W$  down to  $\mu_c$ . However, QCD

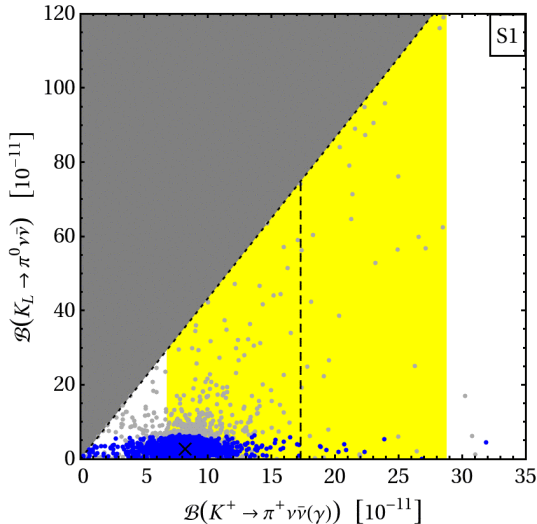


**Figure 3.** Impact of the  $\epsilon'_K/\epsilon_K$  constraint on  $\mathcal{B}(K^+ \rightarrow \pi^+ \nu \bar{\nu}(\gamma))$  and  $\mathcal{B}(K_L \rightarrow \pi^0 \nu \bar{\nu})$ . All points reproduce the quark masses and mixings, and the measured value of  $|\epsilon_K|$ , observables in  $Z^0 \rightarrow b\bar{b}$ , and  $B_d - \bar{B}_d$  mixing. The blue points are consistent with the measured value of  $\epsilon'_K/\epsilon_K$  after varying the hadronic parameters. For details see [20]. The black cross indicates the SM point, the light gray shaded area shows the region excluded by isospin conservation of QCD, and the yellow band displays the experimental 68% CL range.

corrections mainly result from the mixing of  $Q_6$  with current-current operators  $Q_{1,2}$ , and are therefore mostly unaffected by the given high-scale physics. Concerning the electroweak side, in the RS model only contributions to the color-singlet operator  $Q_7$  arise at the scale  $\mu_{\text{KK}}$ , but they are directly fed via operator mixing into  $C_8$  at the scale  $\mu_W$ . Therefore  $\epsilon'_K/\epsilon_K$  in RS is mainly influenced by the electroweak penguin, similar to the decays  $K \rightarrow \pi\nu\bar{\nu}$  where they are the only contributions. For those very decays of charged and neutral Kaons the SM amplitude is tiny, both because of the  $V_{ts}^*V_{td}$  suppression induced by the CKM structure, and the GIM mechanism [24]. The necessary low energy matrix elements for the decays are related to precisely measured semileptonic tree-level decays  $K_{l3}$ . Therefore they offer a very clean test of physics beyond the SM from the theoretical perspective [25], but are likewise challenging to measure. Fortunately two experiments aim to perform measurements with an anticipated accuracy of 10%, namely NA62 (CERN) for the charged mode and Koto (J-PARC) for the neutral mode.

In figure 3 we observe that the RS and SM amplitudes are comparable in size. Indeed, the factors  $F(c_{Q_1})F(c_{Q_2})$  associated with the flavor-violating RS vertex account for approximately the same suppression of  $\lambda^5$  as in the CKM structure of the SM vertex. Moreover, the relevant RS corrections to the left-handed  $s \rightarrow dZ^0$  amplitude have a free phase, in contrast to the small phase in the SM. Since the CP violating neutral mode is proportional to the imaginary part of the contributions, we see that it could in principle obtain large relative corrections, which are however excluded by the following argument. The typical ratio of RS over SM contributions in  $\epsilon'_K/\epsilon_K$  is even a factor of  $\sim 20$  larger than in  $K \rightarrow \pi\nu\bar{\nu}$  case. The reason is well known: The QCD and electroweak penguins cancel in the SM to a large extent, so the value of  $\epsilon'_K/\epsilon_K$  is accidentally small. This entails an effective constraint. The RS amplitude adds linearly and with opposite sign to the SM contribution in  $\epsilon'_K/\epsilon_K$ , and quadratically with the same sign in  $K_L \rightarrow \pi^0\nu\bar{\nu}$ . As the central value of theory prediction for  $\epsilon'_K/\epsilon_K$  is below the experimental one, large enhancements of  $K_L \rightarrow \pi^0\nu\bar{\nu}$  are disfavored already with a conservative treatment of hadronic errors. A lattice determination of the hadronic matrix elements of  $K \rightarrow \pi\pi$ , taking into account the full final state, is in progress [26]. We emphasize that this would be most welcome in view of the constraining potential.

To briefly show one of the many correlations in the  $B$ -meson sector, we select here the decays  $\mathcal{B}(B \rightarrow X_s l^+ l^-)_{q^2 \in [1,6] \text{ GeV}^2}$  and  $\mathcal{B}(B_s \rightarrow \mu^+ \mu^-)$  given in figure 4. After imposing the  $Zb\bar{b}$

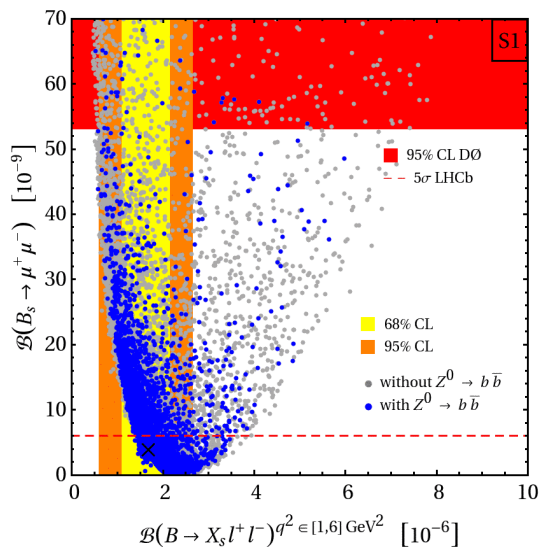


**Figure 4.** Correlation of the prediction for  $\mathcal{B}(B \rightarrow X_s l^+ l^-)$  versus  $\mathcal{B}(B_s \rightarrow \mu^+ \mu^-)$  in the setup with minimal field content. The blue points are consistent with the measured  $Zb\bar{b}$  couplings at the 99% CL. The black cross indicates the SM expectation. For comparison the regions of 68% (yellow) and 95% (orange) CL are also displayed. Furthermore the 95% CL exclusion of  $\mathcal{B}(B_s \rightarrow \mu^+ \mu^-)$  and the minimum branching fraction allowing for a discovery with  $5\sigma$  at LHCb are indicated by the red band and dashed line.

constraint, enhancements in the purely leptonic mode imply values of  $\mathcal{B}(B \rightarrow X_s l^+ l^-)_{q^2 \in [1,6] \text{ GeV}^2}$  safely within the experimentally allowed range in most of the parameter space. This is expected

in models where third generation couplings are most strongly modified [27]. The anti-correlation can be understood by the fact that both modes receive the dominant contribution from axial vector couplings, which are aligned in flavor space, whereas the corresponding SM amplitudes have opposite sign in the two decays. Leptonic  $B$ -meson decays belong to the channels that can be studied by three LHC experiments, ATLAS, CMS, and LHCb. They will probe the branching fraction of  $B_s \rightarrow \mu^+ \mu^-$  down to its SM value and might reveal a signal of new physics well ahead of the direct searches.

We conclude the discussion of flavor observables with a final remark on the changes that occur when the minimal bulk gauge symmetry is extended to a custodial symmetry with left-right parity as mentioned in the introduction. The changes in the couplings have been worked out [14] and the leading effects encoded in flavor-universal rescaling factors. Custodial RS effects in  $Z d_L^i \bar{d}_L^j$  (and  $Z u_R^i \bar{u}_R^j$ ,  $W u_L^i \bar{u}_L^j$ ) couplings are reduced by  $1/L$ , but at the same time increased by a factor of approximately 9 in  $Z d_R^i \bar{d}_R^j$  relative to the minimal RS model. Effects in  $K \rightarrow \pi \nu \bar{\nu}$  decays are therefore typically reduced if  $t_R$  has a natural bulk mass, and large enhancements of  $B_{s,d} \rightarrow \mu^+ \mu^-$  like shown in figure 4 are impossible [28]. The change of the chiral nature of the  $Zsd$  vertex remarkably inverts a correlation found between the branching ratios of  $K^+ \rightarrow \pi^+ \nu \bar{\nu}$  and  $K_L \rightarrow \mu^+ \mu^-$ , but an identification of the chiral structure in this way would require major theoretical progress in the prediction of this radiative decay.

Similarly one can work out the relative coupling shifts for  $\Delta F = 2$  processes, which shows that  $Z'$  exchange is modified by a factor of approximately  $-12$  in  $C_5$ . Although KK-gluon exchange is still dominant in  $K-\bar{K}$  transitions, the  $Z'$  can be competitive in  $B_q-\bar{B}_q$  mixing.

### 3. Consequences for Higgs production and decays

An estimation of the impact of the RS model on Higgs searches at hadron colliders involves first of all the production, where gluon fusion is the main channel. In the SM, the process receives the main contribution from a top-quark triangle loop. After factoring out numerical constants and  $\alpha_s \sqrt{G_F}$  its contribution is encoded in the form factor  $A_q^h(4m_t^2/m_h^2)$ . A small correction arises from the bottom-quark, but since  $A_q^h$  vanishes proportional to its argument the lighter quarks are irrelevant. In the RS model the amplitude for the top-triangle is always reduced but still positive. The origin lies in the modified  $ht\bar{t}$  coupling, which is strongly suppressed ( $\sim -25\%$  for  $M_{KK} = 2$  TeV) because of the compositeness to the top, *i.e.* its IR localization.

Analog to the top triangle all KK modes contribute in triangle diagrams. Since  $A_q^h \rightarrow 1$  in the limit of a very large quark mass, the total sum over all KK fermions appears at first sight to be divergent, as the mass splitting of the higher modes is asymptotically equidistant. However

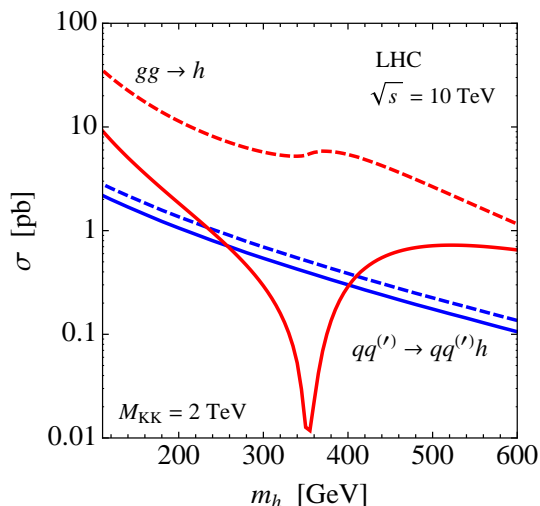


**Figure 5.** Cross sections for the main Higgs-boson production channels at the LHC for a center-of-mass energy of  $\sqrt{s} = 10$  TeV, and  $M_{KK} = 2$  TeV. The dominant channels are gluon-gluon (red) and weak gauge-boson fusion (blue). The dashed lines illustrate the SM predictions, while the solid lines indicate the results obtained in the custodial RS model.

one can show that a delicate cancellation occurs at each KK level between the two chiralities of the vector-like fermion associated to each SM fermion [14]. As a result the sum converges similar to a geometric series instead of diverging like a harmonic series.

Our numerical analysis shown in figure 5 is based on a rescaling of the SM calculation [29]. We find that the relevant amplitudes show only a small spread when scanning over the experimentally allowed RS parameter space. Therefore we display only the median values. The Higgs mass dependence can be easily understood. Up to the  $t\bar{t}$  threshold the form factor increases, but it decreases above. The KK-amplitude is negative and approaches a constant in the heavy Higgs-mass limit. Where it becomes dominant, the full amplitude flips sign, what shows up as a complete destructive interference in the cross section near the  $t\bar{t}$  threshold. Numerically the suppression at the LHC ranges between  $-45\%$  to  $-100\%$  depending on the Higgs mass. At  $M_{\text{KK}} = 3$  TeV the suppression is at most  $-90\%$  and at 5 TeV still up to  $-40\%$ . Thus we obtain a strong sensitivity of the production channel up to high new physics scales.<sup>3</sup> The blue curve in the plot shows the Higgs production via weak gauge-boson fusion which is affected universally by the modified  $WW_h$  vertex and thus reduced by  $-20\%$ . The same factor applies for associated W boson production, and associated top quark pair production is suppressed by  $-40\%$ .

The calculation of the subsequent possible decay modes of the Higgs involves diagrams similar to the production channel, and furthermore gauge boson and KK-gauge boson triangle diagrams for the  $\gamma\gamma$  and  $Z\gamma$  final state. The  $WW_h$  and  $ZZ_h$  couplings experience only a very small reduction. Yet, we recall the reduced production cross section, which renders a detection in the experimentally cleanest mode  $h \rightarrow Z^*Z^* \rightarrow 4l$ , in the region  $m_h > 180$  GeV, to be more difficult. For a lower Higgs mass the decay into two photons is enhanced and can overcome the suppression of the production cross section. The product  $\sigma(gg \rightarrow h)\mathcal{B}(h \rightarrow \gamma\gamma)$  is almost unchanged ( $+3\%$ ) at the scale of  $M_{\text{KK}} = 2$  TeV and  $m_h = 120$  GeV, and even enhanced for a lower new physics scale. However, for an intermediate scale of 3 TeV the cancellation in the production cross section becomes stronger in the low  $m_h$  region, and the product drops severely to 24% of the size expected in the SM.

#### 4. Flavor changing top decays

We end this presentation with a surprising observation about the possible size of flavor changing top decays. For a Higgs coupling to fermions one usually expects factors of the corresponding fermion masses  $m_{q_i}m_{q_j}/v^2$ , stemming from the Yukawa mechanism. Assuming this for the RS model, one would expect the branching ratio of the flavor changing decay  $t \rightarrow ch$ , if kinematically allowed, to be typically two orders of magnitude smaller than for the decay  $t \rightarrow cZ$ .

Models with heavy vector-like quarks can behave differently, if those quarks mix with the SM quarks and additionally couple to the Higgs boson with chiralities opposite to the SM, *i.e.* if the Higgs couples to a heavy left handed singlet and a heavy right handed doublet. Under those conditions an effective operator  $(H^\dagger H)(\bar{Q}_i H^c u_j)$  is induced, which contributes differently to masses and Yukawa couplings [30].

A correct treatment of the Higgs localization in RS shows that, even though heavy “wrong chirality” fermion wave-functions are zero on the IR brane by orbifold boundary conditions, the described type of misalignment exists and contributes to Higgs FCNCs [17]. Numerically this makes the decay  $t \rightarrow ch$  typically even an order of magnitude larger than  $t \rightarrow cZ$ . We show this for a reference Higgs mass  $m_h = 150$  GeV in figure 6, where we also indicate the experimental prospect of detecting the process via the subsequent decay into  $b\bar{b} + \text{jet}$  [31] at later stages of the LHC running. For a lighter Higgs mass of  $m_h = 120$  GeV one multiplies the shown branching ratio with a factor of 4.4. Hence we conclude that misalignment effects astoundingly might lift a detection of the  $htc$  coupling into reach of the LHC.

<sup>3</sup> Note that the numbers have been obtained in the model with custodial gauge symmetry, where the multiplicity of KK-fermion states is higher than in the minimal model.



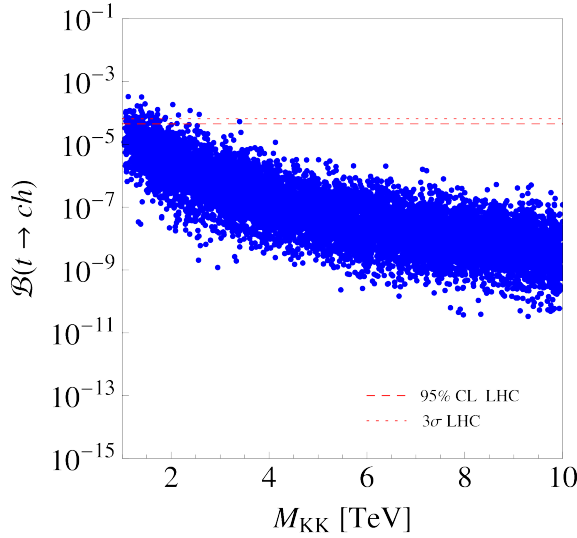


**Figure 6.** Prediction for the branching ratio of the rare decay  $t \rightarrow ch$  in the RS model with extended custodial protection and  $m_h = 150$  GeV. The red dotted (dashed) lines in the plot indicate the expected discovery (exclusion) sensitivities of LHC for  $100 \text{ fb}^{-1}$  integrated luminosity. All points reproduce the correct quark masses, mixing angles, and the CKM phase. In the minimal RS model the constraints from  $Zb\bar{b}$  typically eliminate points with pronounced effects.

## Acknowledgments

It is a pleasure to thank Martin Bauer, Florian Goertz, Uli Haisch, Matthias Neubert and Torsten Pfoh for the fruitful collaboration and the THEP working group of the Johannes-Gutenberg-Universität Mainz for hospitality and partial support during the writeup of this text. I am also grateful to Joachim Brod and Martin Gorbahn for useful comments on the manuscript. This research was supported by the DFG cluster of excellence “Origin and Structure of the Universe”.

## References

- [1] N. Arkani-Hamed and M. Schmaltz, Phys. Rev. D **61**, 033005 (2000)
- [2] L. Randall and R. Sundrum, Phys. Rev. Lett. **83**, 3370 (1999)
- [3] K. Agashe, A. Delgado, M. J. May and R. Sundrum, JHEP **0308**, 050 (2003)
- [4] S. Casagrande, F. Goertz, U. Haisch, M. Neubert and T. Pfoh, JHEP **0810**, 094 (2008)
- [5] Y. Grossman and M. Neubert, Phys. Lett. B **474**, 361 (2000)
- [6] T. Gherghetta and A. Pomarol, Nucl. Phys. B **586**, 141 (2000)
- [7] S. J. Huber, Nucl. Phys. B **666**, 269 (2003)
- [8] K. Agashe, G. Perez and A. Soni, Phys. Rev. D **71**, 016002 (2005)
- [9] M. Blanke, A. J. Buras, B. Duling, S. Gori and A. Weiler, JHEP **0903**, 001 (2009)
- [10] M. S. Carena, A. Delgado, E. Ponton, T. M. P. Tait and C. E. M. Wagner, Phys. Rev. D **68**, 035010 (2003)
- [11] M. Bauer, S. Casagrande, L. Grunder, U. Haisch and M. Neubert, Phys. Rev. D **79**, 076001 (2009)
- [12] M. S. Carena, E. Ponton, J. Santiago and C. E. M. Wagner, Phys. Rev. D **76**, 035006 (2007)
- [13] K. Agashe, R. Contino, L. Da Rold and A. Pomarol, Phys. Lett. B **641**, 62 (2006)
- [14] S. Casagrande, F. Goertz, U. Haisch, M. Neubert and T. Pfoh, JHEP **1009**, 014 (2010)
- [15] T. Aaltonen *et al.* [The CDF Collaboration], arXiv:1101.0034 [hep-ex].
- [16] M. Bauer, F. Goertz, U. Haisch, T. Pfoh and S. Westhoff, JHEP **1011**, 039 (2010)
- [17] A. Azatov, M. Toharia and L. Zhu, Phys. Rev. D **80**, 035016 (2009)
- [18] J. Brod and M. Gorbahn, Phys. Rev. D **82**, 094026 (2010)
- [19] C. Csaki, A. Falkowski and A. Weiler, JHEP **0809**, 008 (2008)
- [20] M. Bauer, S. Casagrande, U. Haisch and M. Neubert, JHEP **1009**, 017 (2010)
- [21] J. Santiago, JHEP **0812**, 046 (2008)
- [22] A. J. Buras, M. Jamin and M. E. Lautenbacher, Nucl. Phys. B **408**, 209 (1993)
- [23] S. Bosch, A. J. Buras, M. Gorbahn, S. Jäger, M. Jamin, M. E. Lautenbacher and L. Silvestrini, Nucl. Phys. B **565**, 3 (2000)
- [24] G. Buchalla and A. J. Buras, Nucl. Phys. B **548**, 309 (1999)
- [25] J. Brod, M. Gorbahn and E. Stamou, arXiv:1009.0947 [hep-ph].
- [26] Q. Liu, RBC and U. collaborations, arXiv:1010.3768 [hep-lat].
- [27] U. Haisch and A. Weiler, Phys. Rev. D **76**, 074027 (2007)
- [28] M. Blanke, A. J. Buras, B. Duling, K. Gemmler and S. Gori, JHEP **0903**, 108 (2009)
- [29] V. Ahrens, T. Becher, M. Neubert and L. L. Yang, Eur. Phys. J. C **62**, 333 (2009)
- [30] F. del Aguila, M. Perez-Victoria and J. Santiago, JHEP **0009**, 011 (2000)
- [31] J. A. Aguilar-Saavedra and G. C. Branco, Phys. Lett. B **495**, 347 (2000)